Stability of the interface between two immiscible fluids over a periodically oscillating flat surface

Krystyna Isakova, Jan Pralits and Rodolfo Repetto
Department of Civil, Chemical and Environmental Engineering, University of Genoa, Italy
E-mail: krystyna.isakova@edu.unige.it, jan.pralits@unige.it, rodolfo.repetto@unige.it

Keywords: Hydrodynamic stability, Stokes layer, dynamics of vitreous substitutes.

SUMMARY. We consider a flat solid surface located at $y^* = 0$, performing sinusoidal oscillations along the x^*–direction, with (x^*, y^*) being a Cartesian system of coordinates. We assume that two immiscible fluids occupy the region of space $y^* \geq 0$. The interface between the two fluids is at $y^* = d^*$; fluid 1 occupies the region $0 \leq y^* \leq d^*$, and fluid 2 extends from d^* to infinity. We study the linear stability of the interface using the normal mode analysis and assuming quasi-steady flow conditions, e.g. assuming that perturbations evolve on a time scale significantly smaller than the period of oscillations of the basic flow. The stability problem leads to two Orr-Sommerfeld equations for the streamfunctions in fluids 1 and 2, coupled with suitable boundary conditions. The resulting eigenvalue problem is solved numerically employing a second order finite-difference scheme and using an inverse iteration approach. The results show that instability of the interface is possible for long enough waves. We study how stability conditions depend on the dimensionless controlling parameters, showing, in particular, the relevant role played by the surface tension between the two fluids.

The work represents a first attempt to understand the instability of the aqueous humour–vitreous substitute instability in vitrectomised eyes. The simple geometrical configuration considered in this work well represents the real case when the thickness of the aqueous layer in contact with the retina is much smaller than the radius of the eye, which is often the case. Our results suggest that shear instability at the aqueous humour–vitreous substitute interface is a plausible mechanism responsible for the onset of emulsification in the vitreous chamber.

1 INTRODUCTION

We consider a flat solid surface, located at $y^* = 0$, performing sinusoidal oscillations along the x^*–direction, see Figure 1. Throughout the paper superscript asterisks denote dimensional variables. We assume that two immiscible fluids occupy the region of space $y^* \geq 0$, the undisturbed position of the interface between the two fluids being located is at $y^* = 0$. We study the linear stability of the interface between the two fluids. For simplicity we assume that the two fluids have the same density and thus focus on shear-induced instability.

The study is motivated by the need of understanding the behaviour of vitreous substitutes injected into the vitreous chamber of the eye after vitrectomy (see Figure $2(a)$). This is a surgical procedure often adopted to treat retinal detachments. With this procedure the vitreous body (the substance that fills the vitreous chamber of the eye), is surgically removed and substituted with "vitreous replacements". Various fluids can be used in vitrectomy procedures, depending on the particular condition of the patient. In this paper we focus on vitreous replacements that are immiscible with water. In this category fall silicon oils, perfluorocarbon liquids and semifluorinated alkane liquids. Mechanical properties, indications for adoption and main complications associated with the existing vitreous substitutes are extensively described in the literature (e.g. [1]).

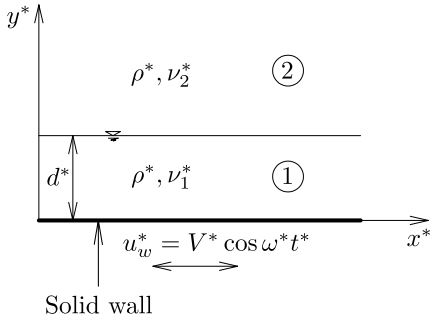

Figure 1: Sketch of the geometry considered and notation.

At present no vitreous replacement fluid exists that can be left indefinitely in the vitreous chamber, since various complications might arise. In particular, vitreous substitutes that are immiscible with water tend to produce an emulsion of droplets in the aqueous. This can lead to various postoperative complications, including cataract, keratopathy, and glaucoma.

In-vivo, owing to the hydrophobic nature of vitreous substitutes, a thin layer aqueous humour (the fluid produced in the anterior part of the eye) is likely to be present between the retina and the vitreous substitute [2]. Emulsification may originate both at the wall (in correspondence of this thin film) [3, 4] and at the tamponade fluid–aqueous free interface where, in the case of incomplete filling of the vitreous chamber, the thickness of the aqueous pocket can be quite large, see Figure 2(b). We focus in this paper on the shear flow instability mechanism that might occur in correspondence of the thin layer separating the vitreous substitute from the retina.

The assumed geometry represents in a highly idealized way the aqueous–vitreous substitute interface in the case in which the thickness of the aqueous layer is much smaller than the eye radius and perturbations are not too long.

The aim of the work is to gather some mechanistic insight on the instability mechanism of the interface between the two fluids, assessing the role that each of the physical quantities involved in the problem has in the instability mechanism, which is regarded as the incipient phase towards emulsification.

2 FORMULATION OF THE MATHEMATICAL PROBLEM

2.1 *Basic flow*

We consider the two immiscible fluids showed in Figure 1 and assume that they are characterised by different kinematic viscosities ν_1^* and ν_2^* and have the same density ρ^*. The flow is induced by periodic motion of the rigid wall located at $y^* = 0$ in the x^*–direction, according to the following time law

$$u_w^* = V^* \cos(\omega^* t^*) = \frac{V^*}{2} \left(e^{i\omega^* t^*} + c.c. \right), \tag{1}$$

where V^* is the amplitude of the oscillations, t^* is time, ω^* is the frequency and $c.c.$ denotes the complex conjugate.

Let $\mathbf{u}_i^*$ be the velocity vector and p_i^* the pressure, where the index i $(= 1, 2)$ identifies the fluid. We scale the problem as follows

$$\mathbf{x} = \frac{\mathbf{x}^*}{d^*}, \quad \mathbf{u}_i = \frac{\mathbf{u}_i^*}{V^*}, \quad p_i = \frac{p_i^*}{\rho^* V^{*2}}, \quad t = \frac{V^*}{d^*} t^*, \quad \omega = \frac{d^*}{V^*} \omega^*. \tag{2}$$

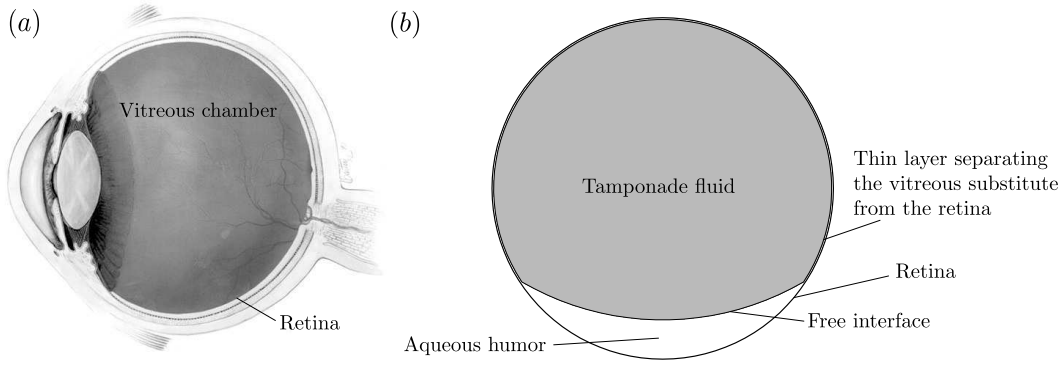

Figure 2: Schematic sketch of a cross-section of an eye (a) and of the vitreous chamber filled with a vitreous replacement fluid (b).

Velocity and pressure are decomposed into a basic state (capital letters) and a perturbation (overlined variables), as follows:

$$\mathbf{u}_i = \mathbf{U}_i + \overline{\mathbf{u}}_i, \quad p_i = P_i + \overline{p}_i. \tag{3}$$

The basic flow is unidirectional, such that $\mathbf{U}_i = [U_i(y,t), 0, 0]$. It can be readily shown that the basic flow pressure is hydrostatic and that the solution for the basic flow velocity reads

$$U_1 = \left(c_1 e^{-ay} + c_2 e^{ay}\right) e^{i\omega t} + c.c., \tag{4a}$$

$$U_2 = c_3 e^{-by} e^{i\omega t} + c.c., \tag{4b}$$

where

$$a = \sqrt{i\omega R}, \tag{5a}$$

$$b = \sqrt{\frac{i\omega R}{m}}, \tag{5b}$$

$$c_1 = \frac{e^{a-b}(a+mb)}{2[e^{a-b}(a+mb) + e^{-a-b}(a-mb)]}, \tag{5c}$$

$$c_2 = \frac{e^{-a-b}(a-mb)}{2[e^{a-b}(a+mb) + e^{-a-b}(a-mb)]}, \tag{5d}$$

$$c_3 = \frac{a}{e^{a-b}(mb+a) + e^{-a-b}(mb-a)}. \tag{5e}$$

In the above expression we have introduced the following dimensionless numbers:

$$R = V^* d^* / \nu_1^*, \quad m = \nu_2^* / \nu_1^*, \tag{6}$$

with R being the Reynolds number characteristic of the flow.

2.2 *The differential system governing the stability*

We now study the stability of the basic flow (4a) and (4b) with respect to infinitesimally small perturbations. Squire's theorem states that, for a steady parallel shear flow, the flow first becomes

unstable to two-dimensional perturbations [5]. Conrad and Criminale [6] showed that the validity of this theorem can be extended to unidirectional unsteady flows. Therefore, we consider two-dimensional perturbations only, so that $\overline{\mathbf{u}}_i = (\overline{u}_i, \overline{v}_i, 0)$, and we introduce the streamfunctions

$$\overline{u}_i = \frac{\partial \psi_i}{\partial y}, \quad \overline{v}_i = -\frac{\partial \psi_i}{\partial x}. \tag{7}$$

In this work we adopt the quasi-steady approach, i.e. we assume that perturbations evolve on a time scale that is significantly smaller than the characteristic scale of the basic flow. This implies that we study the stability of a "frozen" basic flow at time τ, with $0 \leq \tau < 2\pi/\omega$. The suitability of this approach can be verified a posteriori by checking the relative magnitude of the time scale of perturbations with respect to that of the basic flow. Taking advantage of the infinite extension of the domain in the x–direction we expand the unknowns in Fourier modes as follows

$$\psi_i = e^{i\alpha(x-\Omega t)}\hat{\psi}_i(y,\tau) + c.c., \tag{8}$$

where α is the dimensionless wavenumber, the imaginary part of Ω ($\Im(\Omega)$) represents the growth rate of perturbations, while its real part ($\Re(\Omega)$) is the phase velocity.

Moreover, let η denote the dimensionless perturbation of the interface position, measured in units of d^*. We impose

$$\eta = \hat{\eta}(t)e^{i\alpha(x-\Omega t)} + c.c. \tag{9}$$

The equations governing the evolution of the perturbations are then found to be two Orr-Sommerfeld equations that read:

$$\hat{\psi}_1'''' - 2\alpha^2\hat{\psi}_1'' + \alpha^4\hat{\psi}_1 + i\alpha R\left[\hat{\psi}_1\frac{\partial^2 U_1}{\partial y^2} - U_1\left(\hat{\psi}_1'' - \alpha^2\hat{\psi}_1\right)\right] = -i\alpha R\Omega\left(\hat{\psi}_1'' - \alpha^2\hat{\psi}_1\right), \tag{10a}$$

$$\hat{\psi}_2'''' - 2\alpha^2\hat{\psi}_2'' + \alpha^4\hat{\psi}_2 + \frac{i\alpha}{m}R\left[\hat{\psi}_2\frac{\partial^2 U_2}{\partial y^2} - U_2\left(\hat{\psi}_2'' - \alpha^2\hat{\psi}_2\right)\right] = -\frac{i\alpha}{m}R\Omega\left(\hat{\psi}_2'' - \alpha^2\hat{\psi}_2\right), \tag{10b}$$

where the symbol $'$ denotes derivation with respect to y and the basic flow velocity U_i is computed at the generic time τ. The above equations have to be solved subject to the following boundary conditions:

$$\hat{\psi}_1 = 0 \qquad (y=0) \tag{11a}$$

$$\hat{\psi}_1' = 0 \qquad (y=0) \tag{11b}$$

$$U_1\hat{\eta} + \hat{\psi}_1 = \Omega\hat{\eta} \qquad (y=1), \tag{11c}$$

$$\hat{\psi}_1' + \hat{\eta}\frac{\partial U_1}{\partial y} = \hat{\psi}_2' + \hat{\eta}\frac{\partial U_2}{\partial y} \qquad (y=1), \tag{11d}$$

$$\hat{\psi}_1'' + \alpha^2\hat{\psi}_1 + \hat{\eta}\frac{\partial^2 U_1}{\partial y^2} = m\left(\hat{\psi}_2'' + \alpha^2\hat{\psi}_2 + \hat{\eta}\frac{\partial^2 U_2}{\partial y^2}\right) \qquad (y=1), \tag{11e}$$

$$\begin{aligned} &i\alpha R\left(\hat{\psi}_1 U_1' - U_1\hat{\psi}_1'\right) - i\alpha R\left(\hat{\psi}_2 U_2' - U_2\hat{\psi}_2'\right) + \\ &\quad + \left(\hat{\psi}_1''' - 3\alpha^2\hat{\psi}_1'\right) - m\left(\hat{\psi}_2''' - 3\alpha^2\hat{\psi}_2'\right) - i\alpha^3 RS\hat{\eta} = -i\alpha R\Omega\left(\hat{\psi}_1' - \hat{\psi}_2'\right) \qquad (y=1), \end{aligned} \tag{11f}$$

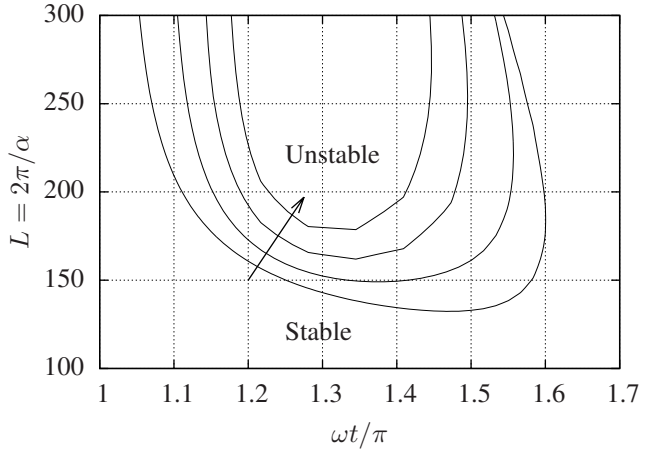

Figure 3: Neutral stability curves in the $L - (\omega t/\pi)$ plane for different values of the parameter m ($m = 5, 10, 15, 20$). The arrow indicates the direction of increase of m. $R = 12$, $\omega = 0.003$, $S = 14$.

$$\hat{\psi}_2 = 0 \qquad (y \to \infty), \tag{11g}$$

$$\hat{\psi}_2' = 0 \qquad (y \to \infty), \tag{11h}$$

where we have introduced the dimensionless surface tension S, defined as $S = \frac{\sigma^*}{\rho^* d^* V^{*2}}$, where σ^* denotes the dimensional surface tension. Note that S is the inverse of the Weber number.

Conditions (11b) and (11a) are the no-slip conditions at the wall. Continuity of the tangential and normal components of the velocity at the interface is enforced by (11c) and (11d). Condition (11e) imposes the continuity of the tangential stress at the interface and (11f) states that the difference between the normal stresses across the interface is balanced by surface tension. Finally, (11g) and (11h) enforce vanishing velocity as $y \to \infty$. Note that, owing to linearisation, the conditions at the interface are imposed in the undisturbed position of the surface, $y = 1$.

The above system of equations can be written as a generalized eigenvalue problem

$$\boldsymbol{A}\hat{\boldsymbol{v}} = \Omega \boldsymbol{B}\hat{\boldsymbol{v}}, \tag{12}$$

where

$$\hat{\boldsymbol{v}} = \left(\hat{\psi}_1, \hat{\eta}, \hat{\psi}_2\right)^T. \tag{13}$$

This is solved numerically employing a second-order finite-difference scheme with uniform discretisation. The eigenvalue problem is solved using an inverse iteration approach. Boundary conditions (11g) and (11h) are enforced using standard asymptotic inviscid solutions.

3 RESULTS

In the following we restrict out attention to a range of values of the controlling parameters that is significant for the ocular application that motivated this study. As baseline values we assume

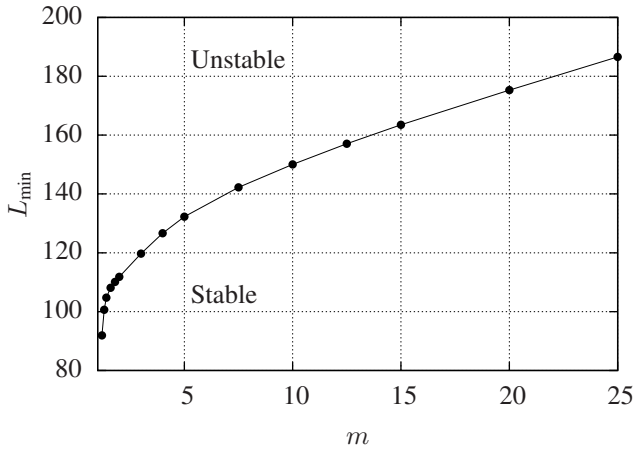

Figure 4: Length of the shortest unstable perturbation $L_{\min}$ versus m. $R = 12$, $\omega = 0.003$, $S = 14$.

$d^* = 5 \times 10^{-5}$ m for the thickness of the layer of fluid 1, and $\sigma^* = 0.05$ N/m for the dimensional surface tension between the two fluids. Considerations of the characteristics of real eye movements (see for instance Becker [7]) allow us to establish relationships between R, ω and S. Vitreous substitutes employed in the surgical practice have viscosities varying within a very wide range of values. Since our main aim is to investigate the role of the mechanical properties of the fluids on the instability mechanism, we vary the parameters m within a fairly large range. Finally, owing to the assumption of quasi-steadiness, we focus on relatively low frequency wall motion. This corresponds to consider large amplitude eye rotations that we assume are more likely to generate instability. We note that in all cases discussed in the following the quantity $\alpha\Re(\Omega)$ (which is a measure of the dimensionless frequency of perturbations) is significantly larger than ω, thus ensuring the separation of time scales required for the quasi-steady approach to be valid.

In Figure 3 we show neutral stability curves, i.e. curves on which $\Im(\Omega) = 0$, on the plane $L - (\omega t/\pi)$, where $L = 2\pi/\alpha$ represents the perturbation wavelength. Each curve corresponds to a different value of the ratio between fluid viscosities m; all other dimensionless parameters are kept fixed. The figure shows that sufficiently long waves are linearly unstable during certain phases of the basic flow cycle. Whether instability will actually occur over long time scales clearly depends on the value of the growth rate and on the initial magnitude of perturbations.

The model shows that as the ratio m between the viscosities of the two fluids increases neutral stability curves shift to longer waves. Thus the system becomes more stable with respect to short perturbations. This is also clearly shown in Figure 4, where the shortest wavelength which is linearly unstable, $L_{\min}$, is plotted versus m.

Figures 5 and 6 show the effect of changing the surface tension parameter S and the Reynolds number R. It appears that decreasing S or increasing R leads to an increased instability of shorter perturbations, the effect of S being particularly strong.

4 DISCUSSION AND CONCLUSIONS

In this paper we have considered the geometry depicted in Figure 1 and studied the linear stability of the interface between the two immiscible fluids 1 and 2, assuming that fluid motion is induced by

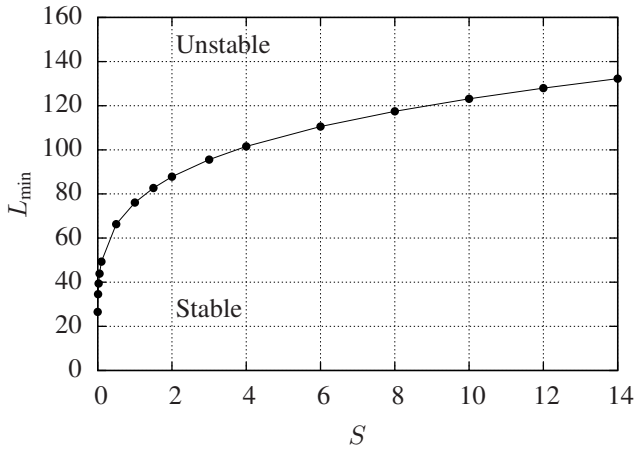

Figure 5: Length of the shortest unstable perturbation $L_{\min}$ versus S. $R = 12$, $\omega = 0.003$, $m = 5$.

periodic oscillations of the solid wall along the x^*–direction, with amplitude V^*/ω^* and frequency ω^*.

The stability analysis shows that long enough waves are linearly unstable during certain phases of the cycle, in the range of the controlling parameters considered. In particular, we find that the shortest unstable wavelength $L_{\min}$

i) grows if the ratio m between the viscosities of the two fluids increases,

ii) decreases if the surface tension parameter S decreases,

iii) decreases if the Reynolds number R increases.

The present work is motivated by the need of understanding the stability conditions of the interface between the aqueous humour layer close to the retina and a vitreous substitute in vitrectomised eyes. We have adopted a highly idealised geometry, which, however, can provide insight on the onset of the aqueous–vitreous substitute interface instability in the case in which the thickness of the aqueous layer is much smaller than the radius of the eye and perturbations are not too long. We note, however, that assuming $d^* = 5 \times 10^{-5}$ m for the thickness of the aqueous layer, the wavelengths found to be unstable are typically small compared to the radius of the eye ($\approx 10^{-2}$ m), especially if small values of the surface tension are considered.

Our results are in qualitative agreement with in-vivo and in-vitro observations of the tendency of vitreous substitutes to produce an emulsion. Indeed, such observations show that:

i) highly viscous vitreous substitutes are more resistant to emulsification than less viscous ones [8, 9, 10];

ii) the presence of surfactants in vitreous substitutes, which decrease the surface tension, promotes instability [11];

iii) patients with increased eye mobility (higher values of R) are more prone to emulsification development.

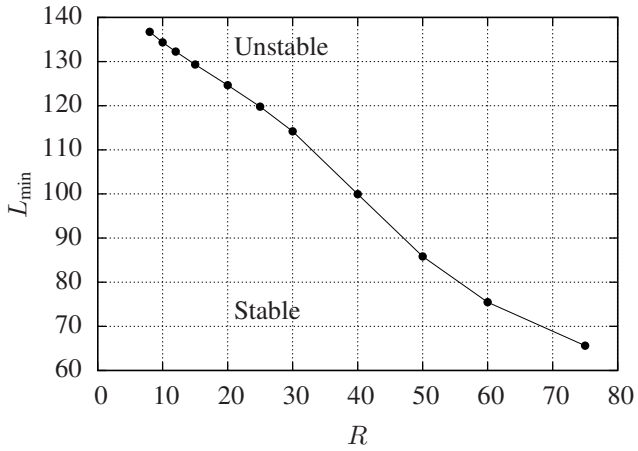

Figure 6: Length of the shortest unstable perturbation $L_{\min}$ versus R. $\omega = 0.003$, $m = 5$, $S = 14$.

Our model allows us to quantify these effects.

Several assumptions underlie the present work, the most relevant of which are listed and briefly commented upon in the following.

i) The model is a poor representation of the real situation in vitrectomised eyes either when the thickness of the aqueous layer is too large or when perturbations are too long. To study the behaviour of long perturbations in the eye additional effects should be accounted for, such as, in particular, the sphericity of the domain and thus wall curvature.

ii) Our stability analysis is based on the quasi-steady approach. In order to account for high frequency oscillations of the wall a stability analysis based Floquet's theory should be adopted.

iii) We assumed that the retina has a perfectly smooth surface. In reality the retinal surface is characterized by a roughness that might enhance the tendency to instability of the aqueous–vitreous substitute interface.

iv) We assumed periodic rotations of the eye. Adoption of a more realistic movements of the wall might have some influence on the results.

v) We focused on the instability mechanism induced by shear between the two fluids. In the case of incomplete filling of the vitreous chamber with the vitreous substitute, emulsification can also be triggered by sloshing of the free interface, see Figure $2(b)$.

References

[1] Kleinberg, T. T., Tzekov, R. T., Stein, L., Ravi, N. and Kaushal, S., "Vitreous Substitutes: A Comprehensive Review", *Survey of Ophthalmology*, **56**, 300–323, 4 (2011).

[2] Winter, M., Eberhardt, W., Scholz, C. and Reichenbach, A., "Failure of potassium siphoning by Mller cells: a new hypothesis of perfluorocarbon liquid-induced retinopathy", *Investigative ophthalmology & visual science*, **41**, 256–261 (2000).

[3] de Silva, D. J., Lim, K. S. and Schulenburg, W. E., "An experimental study on the effect of encircling band procedure on silicone oil emulsification", *The British Journal of Ophthalmology*, **89**, 1348–1350, 10 (2005).

[4] Chan, Y. K., Ng, C. O., Knox, P. C. Garvey, M. J, Williams, R. L. and Wong, D., "Emulsification of silicone oil and eye movements", *Investigative ophthalmology & visual science*, **52**, 9721–9727, 13 (2011).

[5] Squire, H. B., "On the Stability for Three-Dimensional Disturbances of Viscous Fluid Flow between Parallel Walls", *Proceedings of the Royal Society of London. Series A*, **142**, 621–628, 847 (1933).

[6] Conrad, P. W. and Criminale, W. O. "The stability of time-dependent laminar flow: Parallel flows", *Zeitschrift fr angewandte Mathematik und Physik ZAMP*, **16**, 233–254, 2, (1965).

[7] Becker, W. *The neurobiology of saccadic eye movements*, Elsevier Science Publisher BV (Biomedical Division), (1989).

[8] Crisp, A., de Juan, E. and Tiedeman, J., "Effect of silicone oil viscosity on emulsification", *Archives of ophthalmology*, **105**, 546–550, 4, (1987).

[9] Heidenkummer, H. P., Kampik, A. and Thierfelder, S., "Emulsification of silicone oils with specific physicochemical characteristics", *Graefe's Archive for Clinical and Experimental Ophthalmology*, **229**, 88–94, (1991).

[10] Heidenkummer, H. P., Kampik, A. Thierfelder, S., "Experimental evaluation of in vitro stability of purified polydimethylsiloxanes (silicone oil) in viscosity ranges from 1000 to 5000 centistokes", *Retina*, **12**, S28–32, (1992).

[11] Yilmaz, T. and Gler, M., "The role of nystagmus in silicone oil emulsification after pars plana vitrectomy and silicone oil injection for complex retinal detachment", *European journal of ophthalmology*, **18**, 150–154, 1, (2008).